AN IMPLEMENTATION OF THE GROUND STRUCTURE METHOD CONSIDERING BUCKLING AND NODAL INSTABILITIES

BY

TUO ZHAO

THESIS

Submitted in partial fulfillment of the requirements
for the degree of Master of Science in Civil Engineering
in the Graduate College of the
University of Illinois at Urbana-Champaign, 2014

Urbana, Illinois

Advisor:

Professor Glaucio H. Paulino

ABSTRACT

The ground structure method is used to find an optimal solution for the layout optimization problem. The problem domain is discretized with a union of highly connected members, which is called a ground structure. The objective typically is to minimize the total volume of material while satisfying nodal equilibrium constraint and predefined stress limits (plastic formulation). However, such approach may lead to very slender members and unstable nodes that might cause instability issues. This thesis presents the implementation of the ground structure method involving instability consideration. The plastic formulation is implemented considering buckling constraint and nodal instability constraint either in isolation or in combination. The Euler buckling criteria is taken as the buckling constraint in the implementation with local instability consideration. The nominal lateral force method is used in the implementation involving nodal instability consideration. Moreover, the efficiency of the nonlinear programming is addressed. Several numerical examples are presented to illustrate the features of the implementation.

ACKNOWLEDGEMENTS

First and foremost, I would like to express my deepest gratitude to my advisor, Professor Glaucio H. Paulino. It is impossible to finish this work without his guidance and support. His enthusiasm and dedication to research have had a significant impact on me.

I would also like to thank all of my colleagues, Arun Gain, Lauren Beghini, Tomas Zegard, Sofie Leon, Daniel Spring, Junho Chun, Evgueni Filipov, Xiaojia Zhang, Heng Chi, Ke Liu, Maryam Eidini, Peng Wei for their help and support. I'm thankful for Tomas Zegard for many useful suggestions and discussions. Every discussion with him is inspiring and impressive. Additionaly, I am very thankful to my friends: Hao Xu, Xiao Ma, Haoyang Li, Lang Zhou, Qina Yan for their support and encouragement. I also owe my special gratitude to Hao Xu, for providing suggestions and comments on finalizing the document. I would also like to thank Wenting Hou for her continued support, patience and confidence.

Finally, I wish to thank my parents with my deepest gratitude for their unconditional support and love. No words can describe my appreciation for everything they have done for me.

TABLE OF CONTENTS

NOMENCLATURE vi

CHAPTER 1 INTRODUCTION 1

1.1 Literature review addressing stability of optimal structure 5

1.2 Thesis outline and organization 6

CHAPTER 2 PLASTIC FORMULATION 7

2.1 Reformulation into a Linear Programming (LP) problem 7

2.2 Generation of ground structure 8

CHAPTER 3 ON THE GROUND STRUCTURE METHOD WITH BUCKLING CONSTRAINT 10

3.1 Implementation 12

3.2 Verification 13

3.2.1 Single bar column 13

3.2.2 Six bar truss 15

CHAPTER 4 ON THE GROUND STRUCTURE METHOD WITH NODAL INSTABILITY CONSTRAINT 17

CHAPTER 5 ON THE GROUND STRUCTURE METHOD INVOLVING BOTH BUCKLING

AND NODAL INSTABILITY CONSTRAINTS 20

CHAPTER 6 NUMERICAL EXAMPLES 23

6.1 Examples with buckling only consideration 23

6.1.1 Two-dimensional cantilever beam 23

6.1.2 Three-dimensional cantilever beam 28

6.2 Examples with nodal instability only consideration 30

6.2.1 Two-dimensional column 30

6.2.2 Three-dimensional column 31

6.3 An example with both buckling and nodal instability 33

CHAPTER 7 CONCLUSION 35

7.1 Consideration of general domains 36

7.2 Extraction of structures out of the plastic ground structures 36

REFERENCES 37

Nomenclature

$\boldsymbol{B^T}$	Nodal equilibrium matrix
a_i	Cross-sectional area of ith member
l_i	Length of ith member
$\boldsymbol{n}$	A vector with the member internal forces
$\boldsymbol{f}$	Nodal forces excluding the components with supports
V	Optimal volume of the structure
σ_C	Stress limit in compression
σ_T	Stress limit in tension
s^+	Positive slack variables in tension
s^-	Positive slack variables in compression
n_{cr}	Critical Euler buckling load
E	Elastic modulus of the member
I	Moment of inertia of the member
$\boldsymbol{a}$	A vector cross-sectional area
$\boldsymbol{l}$	A vector of length of members
k	Constant depending on the shape of the cross-section area
$\boldsymbol{\sigma^+}$	Tension stress in members
$\boldsymbol{\sigma^-}$	Compression stress in members
$\boldsymbol{\nabla_z f}$	The gradient of the objective function

$\boldsymbol{g}$ Nonlinear constraint

$\boldsymbol{L}(\boldsymbol{z}, \boldsymbol{\lambda})$ Lagrangian function

$\boldsymbol{\nabla_z g}$ Gradient of the nonlinear constraint

$\boldsymbol{\nabla_{zz} L}(\boldsymbol{z}, \boldsymbol{\lambda})$ Derivative of the Lagrangian function

n_{elstic} Elastic member force

a_{opt} Optimal cross-section area

P Applied point loads

V_{opt} Optimal volume of the structure

f_j^x Magnitude of the nominal force in the positive x direction at a given node j

f_j^z Magnitude of the nominal force in the positive z direction at a given node j

m_j Number of bars connected to node j

s_i^- Compressive component of the force in member i

d_i^x Direction cosine of bar i relative to the yz plane which is perpendicular to the direction of f_j^x

r A constant factor which is typically taken as 2%

d_i^z Direction cosine of bar i relative to the xy plane which is perpendicular to the direction of f_j^z

$\boldsymbol{f}^x$ A vector of magnitudes of the nominal lateral forces in the x direction

$\boldsymbol{f}^y$ A vector of magnitudes of the nominal lateral forces in the y direction

$\boldsymbol{f}^z$ A vector of magnitudes of the nominal lateral forces in the z direction

$\boldsymbol{d}^x$ A vector of direction cosines related to yz plane

$\boldsymbol{d^y}$	A vector of direction cosines related to xz plane
$\boldsymbol{d^z}$	A vector of direction cosines related to xy plane
$L_{\boldsymbol{x}}$	Dimension of the domain along x axis
$L_{\boldsymbol{y}}$	Dimension of the domain along y axis
$L_{\boldsymbol{z}}$	Dimension of the domain along z axis

Chapter 1 Introduction

The ground structure (GS) method gives an approximation to a truss layout optimization problem for finding a cost-effective structural framework. It consists of a design domain which is divided into a grid of nodal points interconnected by tentative bars. The union of all or a subset of potential bars is called a ground structure. The objective typically is to minimize the total volume of material while satisfying nodal equilibrium constraint and ensuring that member stresses are within predefined limits. The ground structure method determines the optimal cross-sectional areas for all the bars in the initial ground structure while keeping the nodal locations fixed. As many of the optimal areas will be zero, the optimal framework consists of bars with non-zero cross-sectional areas.

Such typical ground structure method results often contain very slender members and instable nodes, therefore making the structure sensitive to instabilities (Descamps et al., 2014). Figure 1 and Figure 2 show sample problems with instability issues. Slender bars in the compression zone in Figure 1.1(c) may cause a safety issue in practical design (Zegard and Paulino, 2014). In addition, the unstable nodes in Figure 1.2(c) are undesirable.

The consideration of stability issues is meaningful for practical structural design (Pedersen and Nielsen, 2003). Different researchers may use different definition of stability. Tyas et al. (2006) proposed a classification of instability for pin-jointed frameworks.

(a) Local instability occurs when the compressive force in a member exceeds its critical buckling load (Figure 1.3(a)). Euler's formula is considered for general cases.

(b) Nodal instability occurs when a node lying along a compression member lacks lateral bracing (Figure 1.3(b)). The overall or a small section of the structure will fail due to nodal instability.

(c) Global instability occurs when a braced structure buckles as a whole due to insufficient elastic stiffness of the bracing system (Figure 1.3(c)).

This thesis is focusing on the development of the implementation of the ground structure method considering local instability and nodal instability. The global instability might be satisfied for the obtained optimal solution robustly, although this is not considered in the formulation presented here.

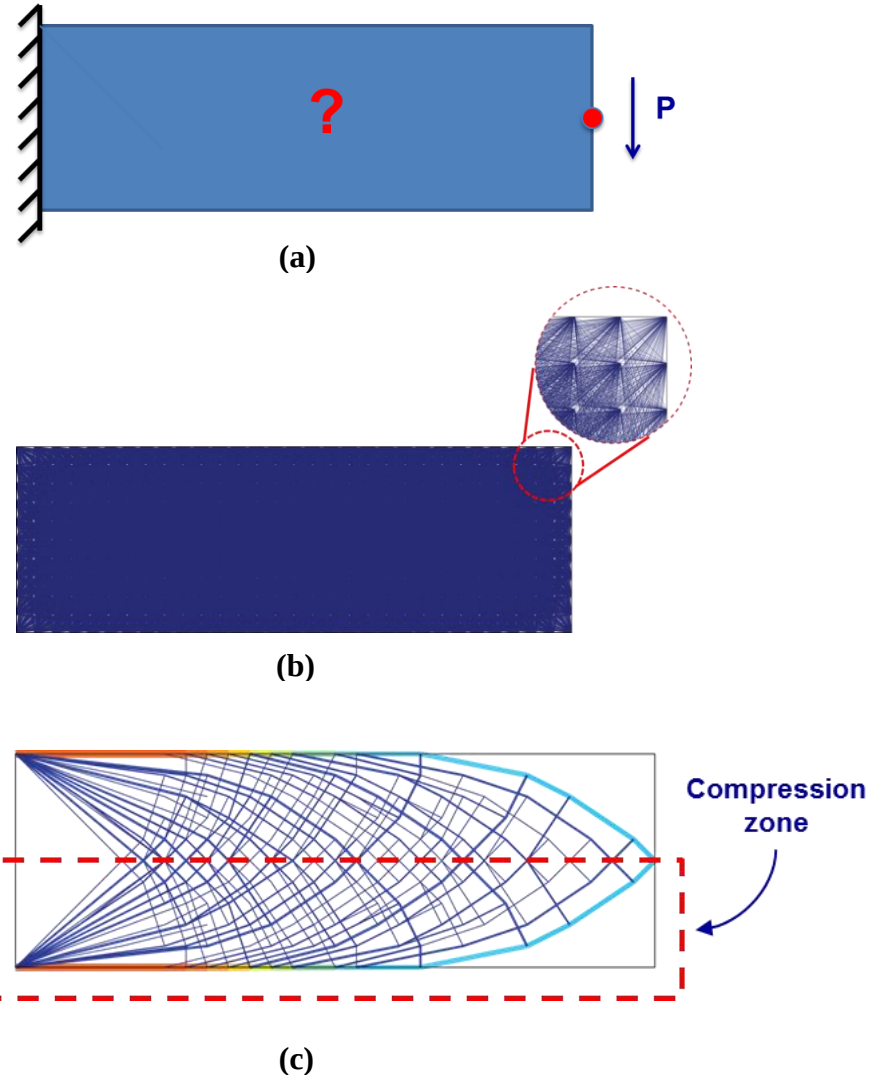

Figure 1.1: A sample cantilever beam problem with local instability issue. (a) Domain, loading and boundary conditions. (b) The initial ground structure with 19632 bars. (c) Solution obtained using typical ground structure method without instability consideration.

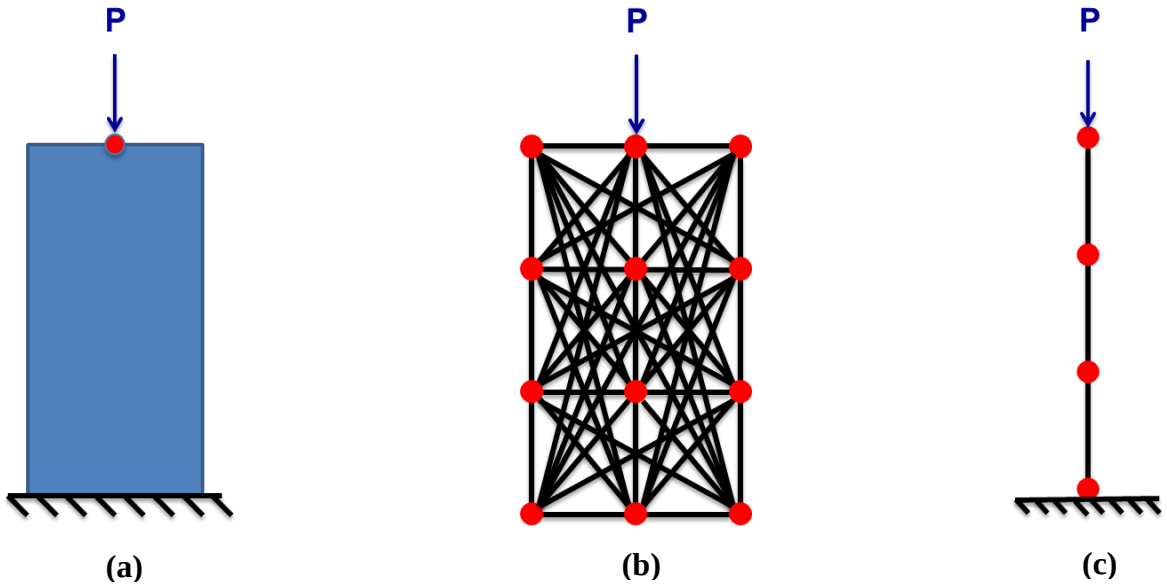

Figure 1.2: A sample column problem with nodal instability issue. (a) Domain, loading and boundary conditions. (b) The initial ground structure with 49 bars. (c) Solution obtained using typical ground structure method without instability consideration.

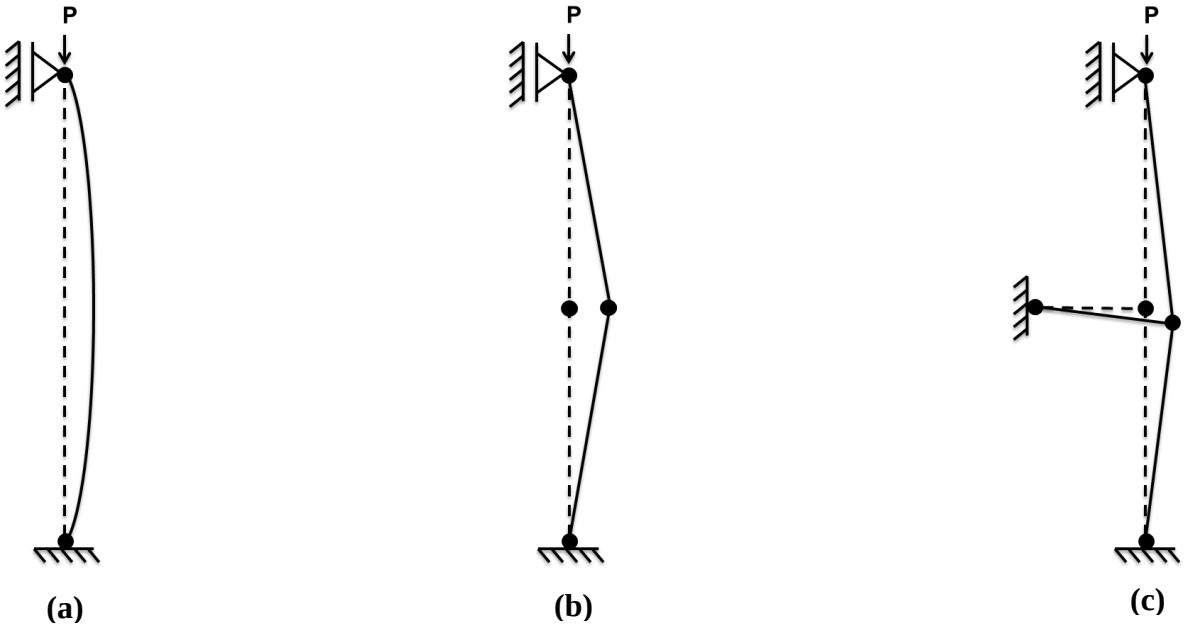

Figure 1.3: Three types of instabilities for pin-jointed frameworks (Descamps et al., 2014). (a) Local instability. (b) Nodal instability. (c) Global instability.

1.1 Literature review addressing stability of optimal structure

Instability issues have drawn lots of attention in the field of layout optimization. Zhou (1996) concluded that topology optimization of trusses with local buckling constraints only may lead to unstable solution with unbraced nodes along compression members. An iterative approach was to eliminate un-braced nodes at the end of the optimization process. However, as Zhou (1996) noted, unstable nodes cancellation may lead to a non-optimal structure because the modified member lengths result in much lower buckling stresses and hence the original design constraints are changed significantly. To solve this problem, Achtziger (1999a,b) developed an unstable nodes cancelation procedure where modified members were considered with consequently lower buckling strength in the optimization process.

An alternative approach is to add system buckling constraints to the formulation to avoid unstable solution (Rozvany,1996). Guo (2005) incorporated the system stability constraint to the stress-constrained minimum volume problem with overlapping bars. A similar method was introduced to the compliance formulation by Ben-Tal et al.(2000) and Kocvara (2002).

The nominal lateral force method is another approach to solve the problem of nodal instability. The method considers small occasional perturbation loadings to closely resemble realistic engineering design problem. Tyas et al. (2006) incorporated nominal lateral force load cases in a linear programming problem formulation to stabilize compression chains. Descamps et al. (2014) adapted the nominal force method to the truss layout optimization comprising the search for optimal nodal locations.

This thesis implements the ground structure method involving stability consideration in three different cases. Case 1 only considers local instability in the implementation of the ground structure method. Euler's buckling formula is formulated in this implementation. Case 2 only considers nodal instability using nominal force method is considered in. Finally, case 3 considers the implementation of ground structure method involving both local instability and nodal instability.

1.2 Thesis outline and organization

The reminder of the thesis is organized as follows. In Chapter 2, the typical ground structure method using plastic formulation is review for minimum volume optimization problem. An effective approach to generate the ground structure for an unstructured domain is also reviewed here. Chapter 3 describes the implementation of the ground structure method considering only buckling constraint. Chapter 4 presents the linear formulation for the implementation of the ground structure method considering nodal instability. Both local and nodal instability are implemented to the ground structure method in Chapter 5. In Chapter 6, several numerical examples for both the two- and three-dimensional domains are presented to highlight the properties of the implementation in Chapters 3, 4 and 5. Finally, the conclusion and summary are given in Chapter 7.

Chapter 2 Plastic formulation

Dorn et al. (1964) developed the ground structure method using plastic formulation for layout optimization problem almost four decades ago. Hemp (1973) proposed a compressive work on plastic formulation extended to multiple load cases. Sokol (2011) optimized the implementation of the ground structure method for orthogonal structured domains. Zegard and Paulino (2014) extended the ground structure method, resulting in an educational and easy-to-use implementation of the truss topology optimization in general non-orthogonal unstructured domains.

To minimize the volume of material such that the stress limits in tension and compression are satisfied, the optimization formulation is given by:

$$\begin{aligned} \min_{\boldsymbol{a},\boldsymbol{n}} \quad & \boldsymbol{V} = \boldsymbol{l}^{\boldsymbol{T}}\boldsymbol{a} \\ \text{s.t.} \quad & \boldsymbol{B}^{\boldsymbol{T}}\boldsymbol{n} = \boldsymbol{f} \\ & -\sigma_C a_i \le n_i \le \sigma_T a_i \\ & a_i \ge 0 \end{aligned} \tag{2.1}$$

where $\boldsymbol{B}^{\boldsymbol{T}}$ is the nodal equilibrium matrix, a_i and l_i are the cross-sectional area and length of the ith member, respectively, $\boldsymbol{n}$ is a vector with the member internal forces, $\boldsymbol{f}$ are nodal forces excluding the components with supports, σ_C is stress limit in compression and σ_T is stress limit in tension.

2.1 Reformulation into a Linear Programming (LP) problem

By introducing positive slack variables s^+ and s^- in the stress constraints, we convert the above inequalities into equalities:

$$
\begin{aligned}
n_i + 2\frac{\sigma_0}{\sigma_C} s_i^- &= \sigma_T a_i \\
-n_i + 2\frac{\sigma_0}{\sigma_T} s_i^+ &= \sigma_C a_i
\end{aligned}
\tag{2.2}
$$

Thus the member cross-sectional area and axial force can be expressed as:

$$
\begin{aligned}
a_i &= \frac{s_i^+}{\sigma_T} + \frac{s_i^-}{\sigma_C} \\
n_i &= s_i^+ - s_i^-
\end{aligned}
\tag{2.3}
$$

Therefore, the optimization problem can be rewritten as:

$$
\begin{aligned}
\min_{\boldsymbol{s^+, s^-}} \quad & \boldsymbol{V = l^T}\left(\frac{\boldsymbol{s^+}}{\boldsymbol{\sigma_T}} + \frac{\boldsymbol{s^-}}{\boldsymbol{\sigma_C}}\right) \\
\text{s.t.} \quad & \boldsymbol{B^T}(\boldsymbol{s^+} - \boldsymbol{s^-}) = \boldsymbol{f} \\
& \boldsymbol{s^+, s^- \geq 0}
\end{aligned}
\tag{2.4}
$$

Because the design variables s^+ and s^- are all positive, the optimization problem becomes a LP problem which can be solved very efficiently using the interior point method (Wright, 2004; Karmarkar, 1984),

2.2 Generation of ground structure

Among other authors, Zegard and Paulino (2014) proposed an efficient way to generate the ground structure without overlapping bars. The level of inter-connectedness of the initial ground structure can be defined as *connectivity level.* Level 1 connectivity will generate bars between all neighboring nodes in the base mesh (Figure 2.1(a)). Level 2 connectivity will generate bars up to the neighbors of the neighbors (Figure 2.1(b)). The bar generation is reaching the full level connectivity (Figure 2.1(c)) when all the nodes were connected with bars.

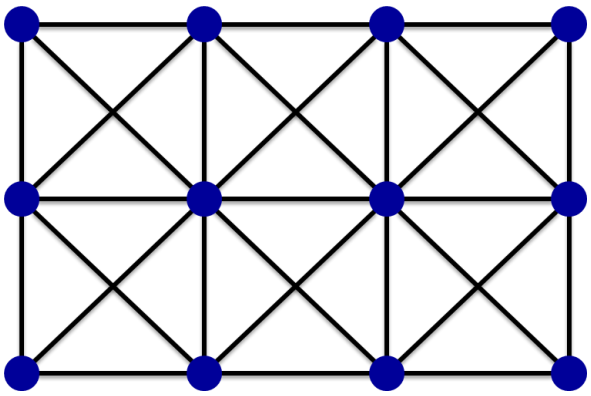

(a)

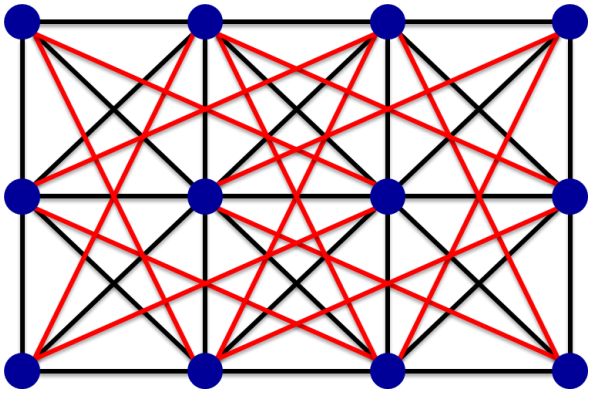

(b)

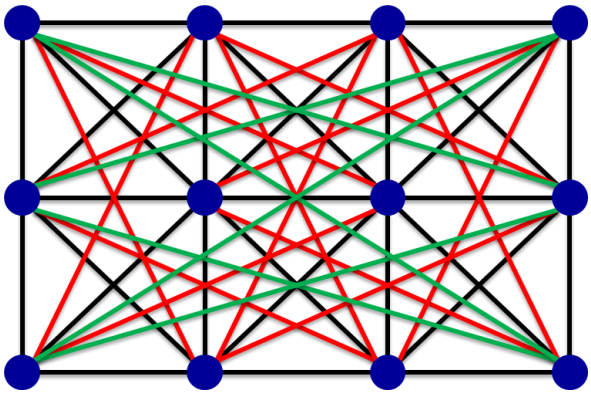

(c)

Figure 2.1: Ground structures with different connectivity levels. (a) Level 1 connectivity. (b) Level 2 connectivity. (c) Full level connectivity.

Chapter 3 On the ground structure method with buckling constraint

The interest in the buckling constraint is reasonable because results of topology optimization using ground structure method often contain very slender members. The effect of local buckling caused by long and slender elements in compression considerably impacts structural safety. The idea is to extend the ground structure method by adding the Euler buckling load constraint in the standard plastic formulation to obtain an optimal structure without any long and slender members.

The critical Euler buckling load of the member can be expressed as

$$n_{cr} = \frac{\pi^2 EI}{l^2} \tag{3.1}$$

where n_{cr} is the critical Euler buckling load of the member, l is the effective buckling length of the member, E is the elastic modulus of the member, and I is the moment of inertia of the member. Because I depends on the shape and size of the cross-section area a of the member, it can be written as $I = \beta a^2$ with a constant factor k depending on the shape of the cross area (Achtziger, 1999a). By letting

$$k = \pi^2 E\beta \tag{3.2}$$

the critical buckling load can be rewritten as

$$n_{cr} = k\frac{a^2}{l^2} \tag{3.3}$$

For instance, $k = \pi E/4$ when the cross-section of the member is a circle, and $k = \pi^2 E/12$ when the cross-section of the member is a square.

An intuitive way to consider bucking instability in the ground structure method is to add the critical

Euler buckling load as a constraint in the plastic formulation. Then the formulation (2.4) can be reformulated as

$$\begin{aligned} \min_{\boldsymbol{s^+},\, \boldsymbol{s^-},\, \boldsymbol{a}} \quad & \boldsymbol{V} = \boldsymbol{l^T a} \\ s.t. \quad & \boldsymbol{B^T}(\boldsymbol{s^+} - \boldsymbol{s^-}) = \boldsymbol{f} \\ & \boldsymbol{s^-} \leq \boldsymbol{n_{cr}} = k\frac{\boldsymbol{a}^2}{l^2} \\ & \boldsymbol{a} \geq \frac{\boldsymbol{s^+}}{\boldsymbol{\sigma_T}} + \frac{\boldsymbol{s^-}}{\boldsymbol{\sigma_C}} \\ & \boldsymbol{a} \geq \boldsymbol{0} \\ & \boldsymbol{s^+}, \boldsymbol{s^-} \geq \boldsymbol{0} \end{aligned} \tag{3.4}$$

The objective is to minimize the volume of the material. The design variables are member forces in compression $\boldsymbol{s^-}$, member forces in tension $\boldsymbol{s^+}$, and cross-section area $\boldsymbol{a}$. Note that the formulation becomes non-linear because of the non-linear buckling constraint. This constraint is related to the number of bars in the ground structure method. The efficiency of the implementation of this non-linear formulation might be low because of the usually high number of bars presented in the ground structure. *Thus, it is better to linearize the buckling constraint term to improve the efficiency of the implementation*. Instead of using member force, let's introduce stress in the members as the design variables

$$\begin{aligned} \boldsymbol{\sigma^+} &= \frac{\boldsymbol{s^+}}{\boldsymbol{\sigma_T}} \\ \boldsymbol{\sigma^-} &= \frac{\boldsymbol{s^-}}{\boldsymbol{\sigma_C}} \end{aligned} \tag{3.5}$$

Then the formulation (3.4) can be reformulated with a linearized buckling constraint term, shown as follows:

$$\begin{aligned} \underset{\boldsymbol{\sigma}^+,\,\boldsymbol{\sigma}^-,\,a}{min} \quad & \boldsymbol{V} = \boldsymbol{l}^{\boldsymbol{T}}\boldsymbol{a} \\ s.t. \quad & \boldsymbol{B}^{\boldsymbol{T}}(\boldsymbol{\sigma}^+ - \boldsymbol{\sigma}^-)\boldsymbol{a} = \boldsymbol{f} \\ & \boldsymbol{\sigma}^- \leq \boldsymbol{\sigma}_{\boldsymbol{cr}} = k\frac{\boldsymbol{a}}{l^2} \\ & \mathbf{0} \leq \boldsymbol{\sigma}^+ \leq \boldsymbol{\sigma}_{\boldsymbol{T}} \\ & \mathbf{0} \leq \boldsymbol{\sigma}^- \leq \boldsymbol{\sigma}_{\boldsymbol{C}} \\ & \boldsymbol{a} \geq \mathbf{0} \end{aligned} \tag{3.6}$$

Equation (3.6) is the proposed formulation for the implementation of the ground structure method considering buckling constraint. This, from now on, the formulation (3.4) is not considered anymore.

3.1 Implementation

The nonlinear formulation (3.6) was implemented in MATLAB using its pre-defined function which is called "*fmincon*". Although many algorithms can be used to solve a nonlinear programming, strong algorithmic differences exist (Descamps et al., 2014). Our numerical examples have shown that the interior-point method exhibits good performance because of its efficiency on handling large, sparse problems. To increase the accuracy and save the computational time, gradient and Hessian information are supplied. The gradient of the objective function is given by

$$\boldsymbol{\nabla_z f} = \left[\boldsymbol{\nabla_a f}\ \ \boldsymbol{\nabla_{\sigma^+} f}\ \ \boldsymbol{\nabla_{\sigma^-} f}\right]^{\boldsymbol{T}} \tag{3.7}$$

where the vector collecting the optimization variables is $\boldsymbol{z} = \left[\boldsymbol{a}\ \ \boldsymbol{\sigma}^+\ \ \boldsymbol{\sigma}^-\right]^{\boldsymbol{T}}$. The gradient of the nonlinear constraint is shown as

$$\boldsymbol{\nabla_z g} = \left[\boldsymbol{\nabla_a g}\ \ \boldsymbol{\nabla_{\sigma^+} g}\ \ \boldsymbol{\nabla_{\sigma^-} g}\right]^{\boldsymbol{T}} \tag{3.8}$$

In addition, the hessian matrix is given by the second derivative of the Lagrangian function as

follows

$$\nabla_{zz}^{2} L(z, \lambda) = \nabla^2 f(z) + \sum \lambda_i \nabla^2 g_i(z) \tag{3.9}$$

All the gradient and Hessian matrixes in the implementation code were tested by Finite Difference Method (Haftka and Gurdal, 1992).

3.2 Verification

By studying two simple illustrative examples in details, the accuracy of the implementation is verified and an intuitive idea about how buckling constraint will affect the optimum solution is gained. In either of the two examples, the structure has the elastic modulus $E = 1$, stress limits in tension and compression $\sigma_T = 0.2$ and $\sigma_C = 0.2$, respectively, applied force $P = 1$ (consistent units are employed) and circular cross section with $k = \pi E/4$.

3.2.1 Single bar column

A single bar column example with a point load P is shown in Figure 3.1 with indication of boundary conditions and dimension of the structure. The objective is to minimize volume of the structure while considering local stress limit and buckling constraint. The analytical solution of the problem can be obtained. The critical buckling load in the column is given by

$$n_{cr} = \frac{\pi^2 EI}{l^2} = k\frac{a^2}{l^2} \tag{3.10}$$

The elastic member force can be expressed as

$$n_{elstic} = \sigma_C a \tag{3.11}$$

Then the optimal cross section area is

$$a_{opt} = \max\left\{\sqrt{\frac{PL^2}{k}},\ \frac{P}{\sigma_C}\right\} \tag{3.12}$$

Finally the optimal volume of the structure is obtained by

$$V_{opt} = a_{opt} l \tag{3.13}$$

Given different magnitudes of the applied load, the analytical optimal volume is compared with that obtained from the implementation in this section (Figure 3.2). The comparison shows that the accuracy of the implementation is very good.

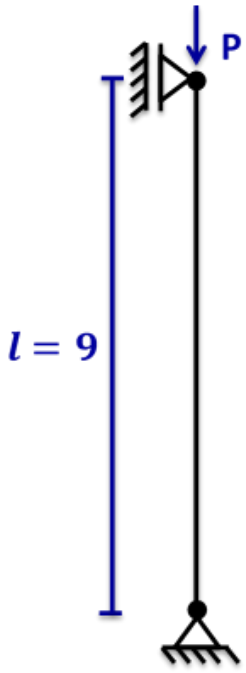

Figure 3.1: A verification example with a single bar column.

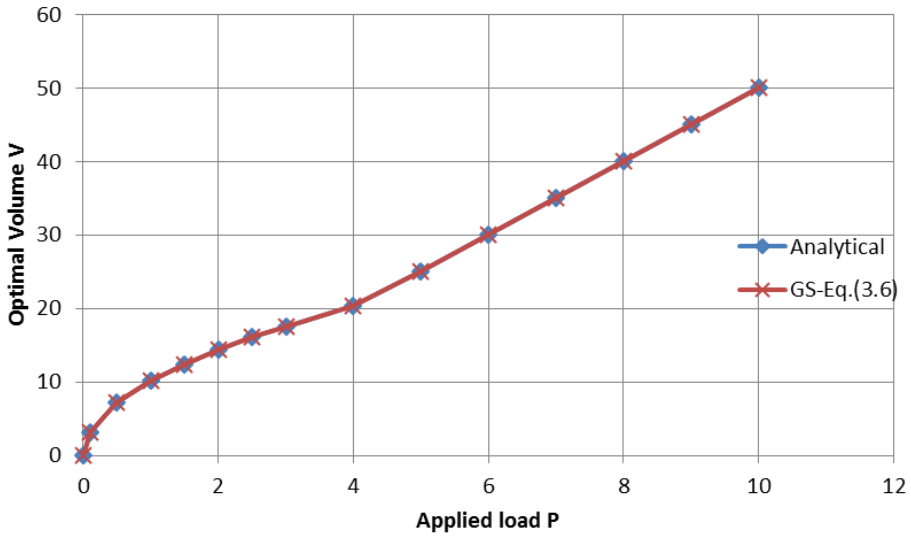

Figure 3.2: Comparison of the optimal volume between analytical solution and GS implementation.

3.2.2 Six bar truss

In order to gain some intuitive insight into the optimal topology of truss design under buckling constraints, a six bar truss volume minimization problem is investigated. The six bar truss with a point load $P = 1$ is shown in Figure 3.3(a) with indication of boundary condition and dimension of the structure. If buckling instability is not considered, the optimal topology is a long and slender bar in compression, as shown in Figure 3.3(b). However, the optimal structure (Figure 3.3(c)) is composed of five shorter members if stability consideration is implemented. In this figure, bars in red denote compression members, and bars in blue denote tension members. With buckling instability consideration, the topology changes according to the angle. There is a critical angle for the change of topology. When the angle of α is more than 69 degrees, the topology is a combination of five shorter bars. The topology becomes a single bar when the angle of α is less than 69 degrees.

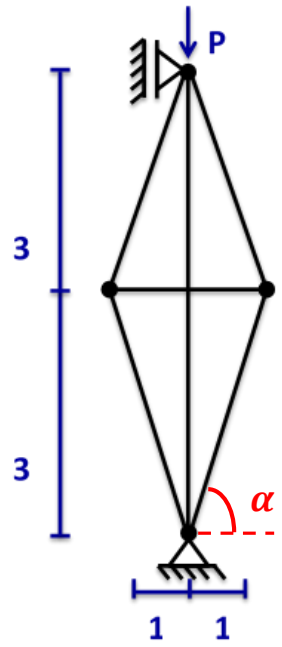

(a)

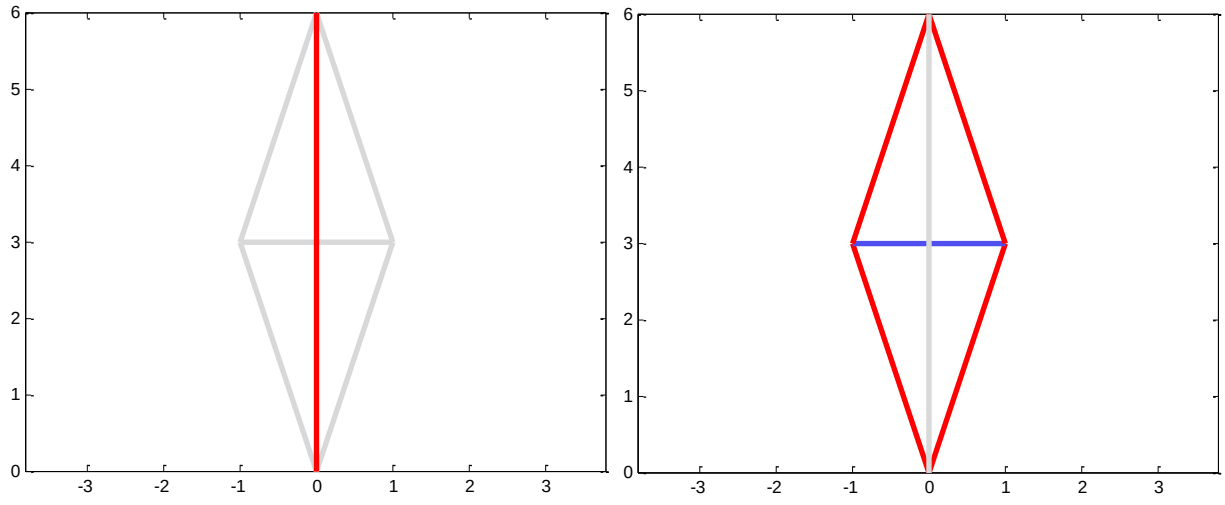

(b) **(c)**

Figure 3.3: A six bar truss verification example. (a) Domain with loads, boundary conditions and dimensions (a) Optimum solution without stability consideration. (b) Optimum solution with stability consideration. Notation: blue denotes tension and red denotes compreesion.

Chapter 4 On the ground structure method with nodal instability constraint

The nominal lateral force method was studied by Winter (1958) for design of bracing systems. Tyas et al. (2006) adapted the method to layout optimization using the ground structure method. Lateral force perturbations were applied to non-stabilized nodes in compression members so that additional structural braces are used to ensure stability of the internal node. The direction of the lateral forces is in the plane perpendicular to that in which the member force is in compression (Figure 4.1(a)). The magnitude of the lateral force is typically 2% of the compressive force that is being resisted (Tyas et al., 2006). For instance, at a given node j, the magnitude of the nominal force in the positive x direction, f_j^x (Figure 4.1(b)) , can be expressed as

$$f_j^x = r\sum_{i=1}^{m_j} s_i^- d_i^x \tag{4.1}$$

where m_j is the number of bars connected to node j, s_i^- is the compressive component of the force in member i, d_i^x is the direction cosine of bar i relative to the yz plane which is perpendicular to the direction of f_j^x and r is a constant factor which is typically taken as 2%. The nominal force in the positive z direction, f_j^z(Figure 4.1(c)), can be calculated in the similar way

$$f_j^z = r\sum_{i=1}^{m_j} s_i^- d_i^z \tag{4.2}$$

The only difference is that d_i^z is the direction cosine of bar i relative to the xy plane which is perpendicular to the direction of f_j^z. In a similar manner, the nominal force in the y direction can

be calculated using the direction cosine related to the xz plane.

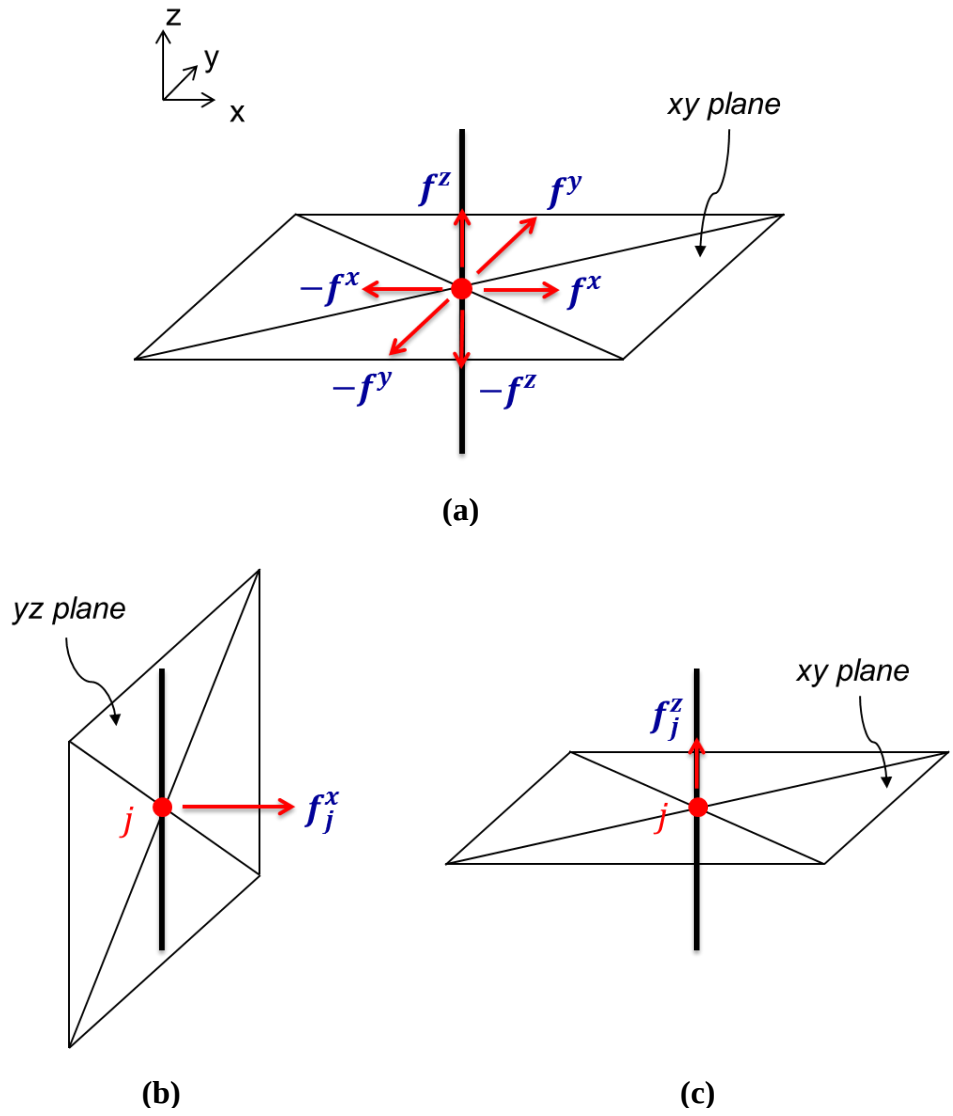

Figure 4.1: The nominal lateral force method (Tyas et al., 2006). (a) Directions of the nominal forces. (b) The nominal force in positive x direction. (c) The nominal force in positive z direction.

Recall the linear programming plastic formulation for minimum volume optimization problem in ground structure method:

$$\begin{aligned} \underset{s^+,\, s^-}{min} \quad & \boldsymbol{V = l^T a} \\ s.t. \quad & \boldsymbol{B^T(s^+ - s^-) = f} \\ & \boldsymbol{a = \frac{s^+}{\sigma_T} + \frac{s^-}{\sigma_C}} \\ & \boldsymbol{s^+, s^- \geq 0} \end{aligned} \tag{4.3}$$

To take the nodal instability into consideration, six new equilibrium constraints related to nominal lateral load cases are required. Thus these constraints are included with additional constraints defining the magnitudes of the nominal forces into the program. The formulation can be written as

$$\begin{aligned} \underset{s^+,\, s^-,\, a}{\boldsymbol{min}} \quad & \boldsymbol{V = l^T a} \\ \boldsymbol{s.t.} \quad & \boldsymbol{B^T(s^{0+} - s^{0-}) = f} \\ & \boldsymbol{B^T(s^{\alpha+} - s^{\alpha-}) = f_n^\alpha} \\ & \boldsymbol{f_n^\alpha \geq r s^0 d_n^\alpha} \\ & \boldsymbol{a \geq \frac{s^+}{\sigma_T} + \frac{s^-}{\sigma_C}} \\ & \boldsymbol{s^+, s^- \geq 0} \\ & \boldsymbol{a \geq 0} \\ & \boldsymbol{\alpha = 1, \ldots 6} \end{aligned} \tag{4.4}$$

where $\boldsymbol{f_n^\alpha = \{f^x, -f^x, f^y, -f^y, f^z, -f^z\}^T}$, $\boldsymbol{d_n^\alpha = \{d^x, d^y, d^z\}^T}$, $\boldsymbol{s^{\alpha+} = \{s^{1+}, s^{2+}, s^{3+}, s^{4+}, s^{5+}, s^{6+}\}^T}$, $\boldsymbol{s^{\alpha-} = \{s^{1-}, s^{2-}, s^{3-}, s^{4-}, s^{5-}, s^{6-}\}^T}$, $\boldsymbol{s^+ = \{s^{0+}, s^{\alpha+}\}^T}$ and $\boldsymbol{s^- = \{s^{0-}, s^{\alpha-}\}^T}$. $\boldsymbol{f^x}$, $\boldsymbol{f^y}$, $\boldsymbol{f^z}$ are magnitudes of the nominal lateral forces in the x, y and z directions; and $\boldsymbol{d^x}$, $\boldsymbol{d^y}$ and $\boldsymbol{d^z}$ are direction cosine related to yz, xz and xy planes, respectively. *Note that Eq. (4.4) involving nodal instability constraints is a linear programming formulation*.

Chapter 5 On the ground structure method involving both buckling and nodal instability constraints

In the previous chapters 3 and 4, buckling constraint and nodal instability constraint are implemented separately into the ground structure method. Both of those two instability constraints are considered simultaneously in the implementation of the ground structure method in this chapter.

Recall the linear programming formulation considering nodal instability only

$$\begin{aligned} \min_{s^+, s^-, a} \quad & V = l^T a \\ s.t. \quad & B^T(s^{0+} - s^{0-}) = f \\ & B^T(s^{\alpha+} - s^{\alpha-}) = f_n^\alpha \\ & f_n^\alpha \geq r s^0 d_n^\alpha \\ & a \geq \frac{s^+}{\sigma_T} + \frac{s^-}{\sigma_C} \\ & s^+, s^- \geq 0 \\ & a \geq 0 \\ & \alpha = 1, \dots 6 \end{aligned} \tag{5.1}$$

The Euler's critical buckling load can be written as

$$n_{cr} = k\frac{a^2}{l^2} \tag{5.2}$$

An intuitive idea to consider both nodal and buckling simultaneously is to add Euler's critical load constraint into the above formulation directly. Then (5.1) can be reformulated as

$$
\begin{aligned}
\min_{s^+, s^-, a} \quad & V = l^T a \\
s.t. \quad & s^- \le n_{cr} = k\frac{a^2}{l^2} \\
& B^T(s^{0+} - s^{0-}) = f \\
& B^T(s^{\alpha+} - s^{\alpha-}) = f_n^\alpha \\
& f_n^\alpha \ge r s^0 d_n^\alpha \\
& a \ge \frac{s^+}{\sigma_T} + \frac{s^-}{\sigma_C} \\
& s^+, s^- \ge 0 \\
& a \ge 0 \\
& \alpha = 1, \dots 6
\end{aligned}
\tag{5.3}
$$

Note that the formulation becomes non-linear because of the non-linear buckling constraint. This constraint is related to the number of bars in the ground structure method. The efficiency of the implementation of this non-linear formulation might be very low because of the large number of bars generated in the ground structure. Thus, it is better to linearize the buckling constraint term to improve the efficiency of the implementation. Let's introduce member stress σ^+ and σ^- as another new design variables. Then the buckling constraint can be rewritten as

$$
\begin{aligned}
& B^T(\sigma^+ - \sigma^-)a = f \\
& \sigma^- \le \sigma_{cr} = k\frac{a}{l^2} \\
& 0 \le \sigma^+ \le \sigma_T \\
& 0 \le \sigma^- \le \sigma_C
\end{aligned}
\tag{5.4}
$$

Using the reformulated buckling constraint, we obtain the formulation including both local and nodal instability constraints

$$
\begin{aligned}
\min_{\sigma^+,\,\sigma^-,\,s^+,\,s^-,\,a} \quad & V = l^T a \\
s.t. \quad & B^T(\sigma^+ - \sigma^-)a = f \\
& \sigma^- \le \sigma_{cr} = k\frac{a}{l^2} \\
& 0 \le \sigma^+ \le \sigma_T \\
& 0 \le \sigma^- \le \sigma_C \\
& B^T(s^{0+} - s^{0-}) = f \\
& B^T(s^{\alpha+} - s^{\alpha-}) = f_n^\alpha \\
& f_n^\alpha \ge r s^0 d_n^\alpha \\
& a \ge \frac{s^+}{\sigma_T} + \frac{s^-}{\sigma_C} \\
& s^+, s^- \ge 0 \\
& a \ge 0 \\
& \alpha = 1, \dots 6
\end{aligned}
\tag{5.5}
$$

This is the main and most complete formulation adopted in the present work.

Chapter 6 Numerical examples

In this chapter, several numerical examples clarify the effects of buckling, nodal and combined instability considerations. In every example, the tension limit and compression limit are taken as 0.2. The cross-section of the member is circular with $k = \pi E/4$. Consider elastic modulus as unit. In section 6.1, a cantilever beam problem is considered to investigate the effect of buckling instability consideration in the implementation of the ground structure method. Both two- and three-dimensional ground structures are generated. In section, 6.2, a column problem is proposed to illustrate nodal instability. Section 6.3 is concerned with the implementation of the ground structure involving both buckling and nodal instability.

6.1 Examples with buckling only consideration

6.1.1 Two-dimensional cantilever beam

The cantilever beam is fixed at one end, and loaded at the center of the other end (Figure 6.1). The domain has dimensions with $L_x = 3$ and $L_y = 1$. The magnitude of the load is 1. The domain is discretized with 6×2, 12×4, 18×6, 24×8 and 30×10 mesh separately. Figure 6.2 and Figure 6.3 show the different optimum topologies for the problem with different mesh. All the data are collected in Table 6.1 in terms of number of element in base mesh N_e, number of node in base mesh N_n, level connectivity Lvl, number of bars N_b and optimal volume V.

The convergence behavior of the implementation considering buckling constraint is shown in Figure 6.4 with red line. As a comparison, the behavior of the ground structure method without

instability consideration for the same problem is plotted as blue line.

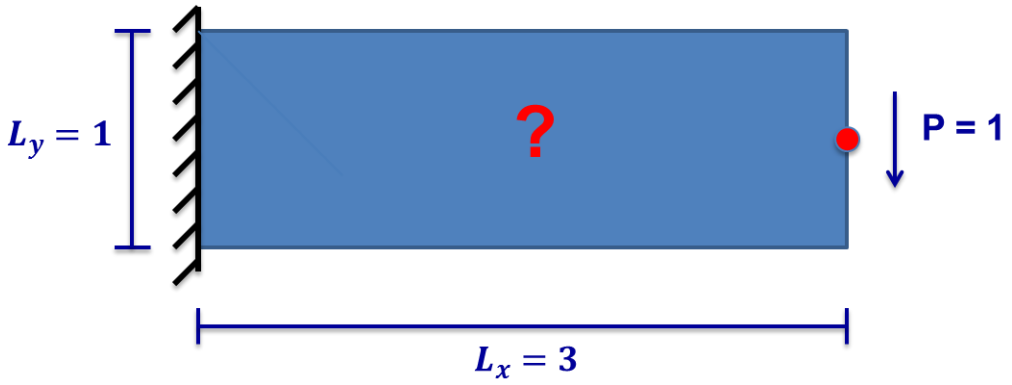

Figure 6.1: A cantilever beam problem. Domain with loads, boundary conditions and dimensions.

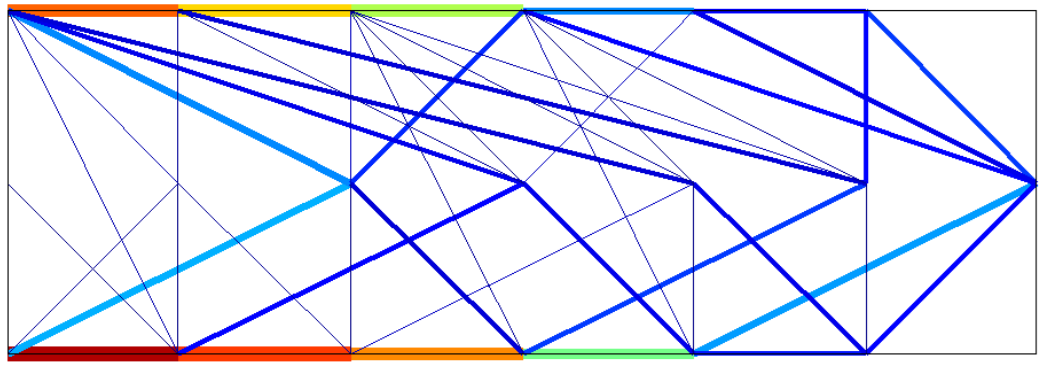

(a)

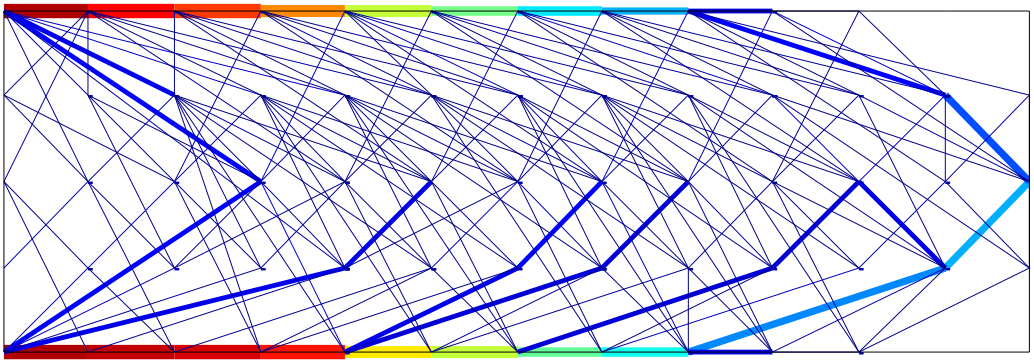

(b)

Figure 6.2: Final topologies for the cantilever beam problem. (a) 6×2 mesh with level 4 connectivity $\rightarrow$ 124 bars. (b) 12×4 mesh with level 4 connectivity $\rightarrow$ 752 bars.

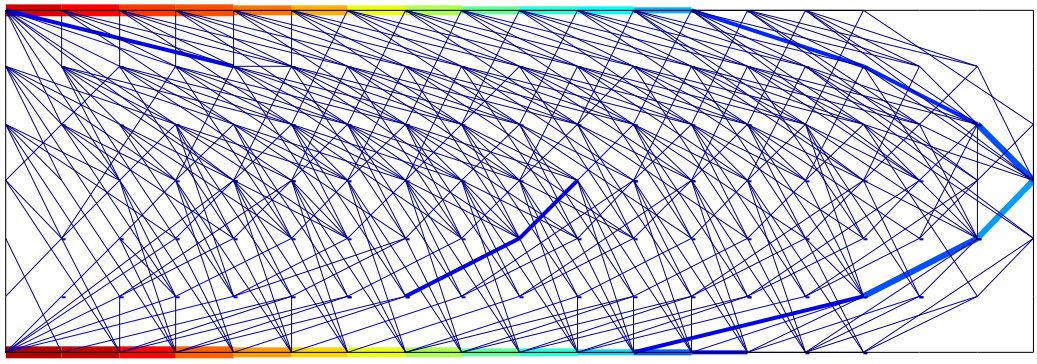

(a)

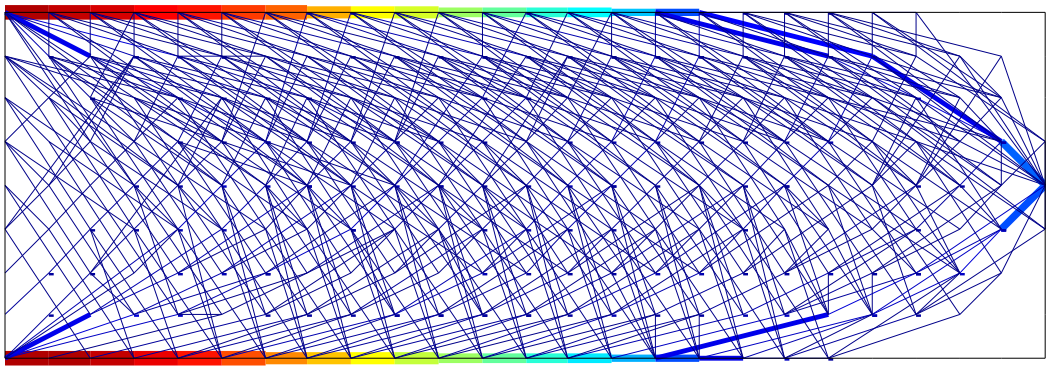

(c)

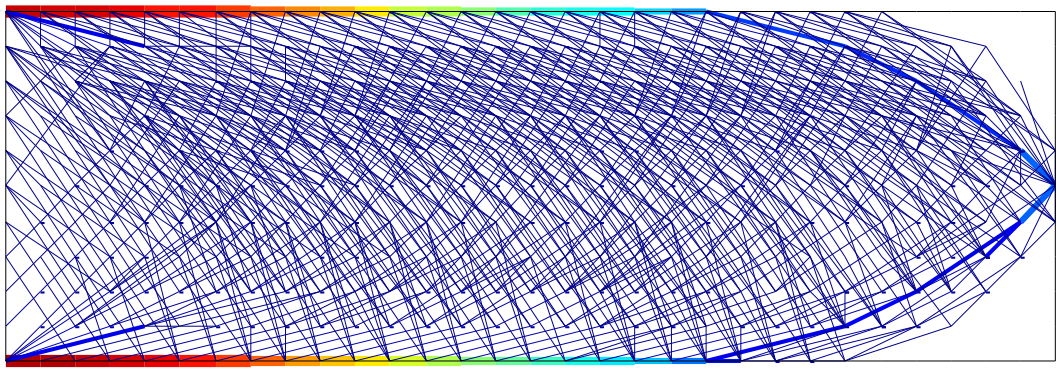

(c)

Figure 6.3: Final topologies for the cantilever beam problem. (a) 18×6 mesh with level 4 connectivity $\rightarrow$ 1976 bars. (b) 24×8 mesh with level 4 connectivity $\rightarrow$ 3776 bars. (c) 30×10 mesh with level 4 connectivity $\rightarrow$ 6152 bars.

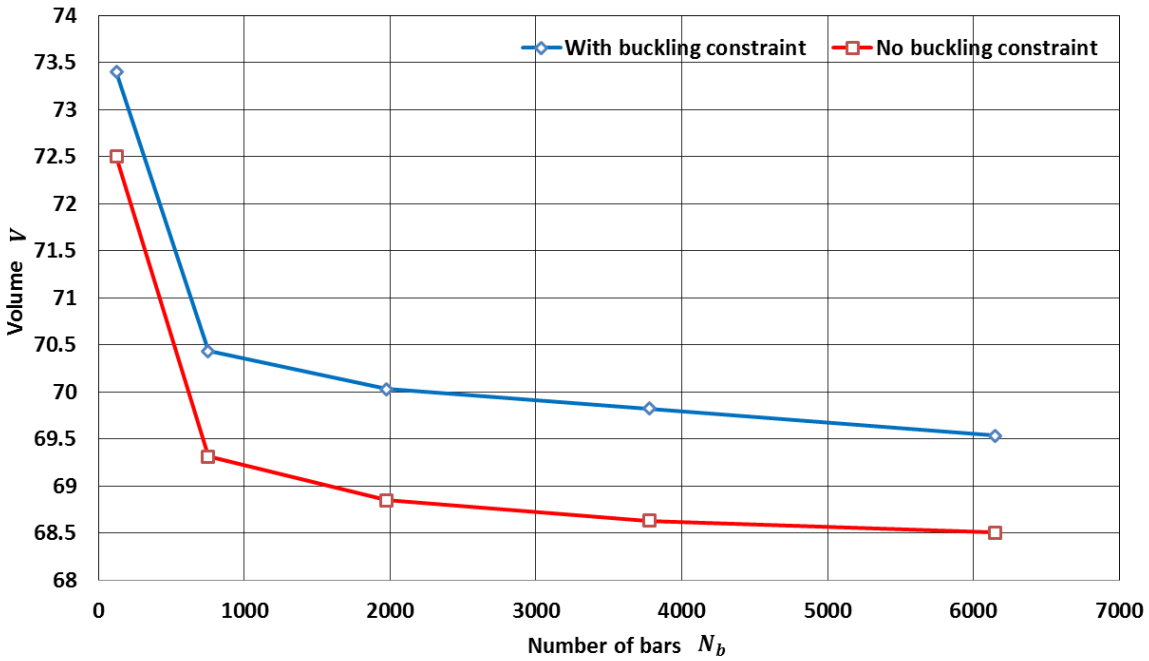

Figure 6.4: Comparison of the convergence rate for the cantilever beam problem

Table 6.1: Summary of results for the implementation with buckling constraint

N_e	N_n	Lvl	N_b	V
12	21	4	124	73.3995
48	65	4	752	70.4341
108	133	4	1976	70.029
192	225	4	3776	69.8242
300	341	4	6152	69.5379

Figure 6.5 shows the comparison of optimal topologies between the implementation considering buckling and that not considering instability issue. Same mesh and connectivity level of the ground structure (Figure 6.5(a)) is used in the comparison. The optimal topology without instability

consideration is shown in Figure 6.5(b). Moreover, Figure 6.5(c) shows the final result with buckling consideration.

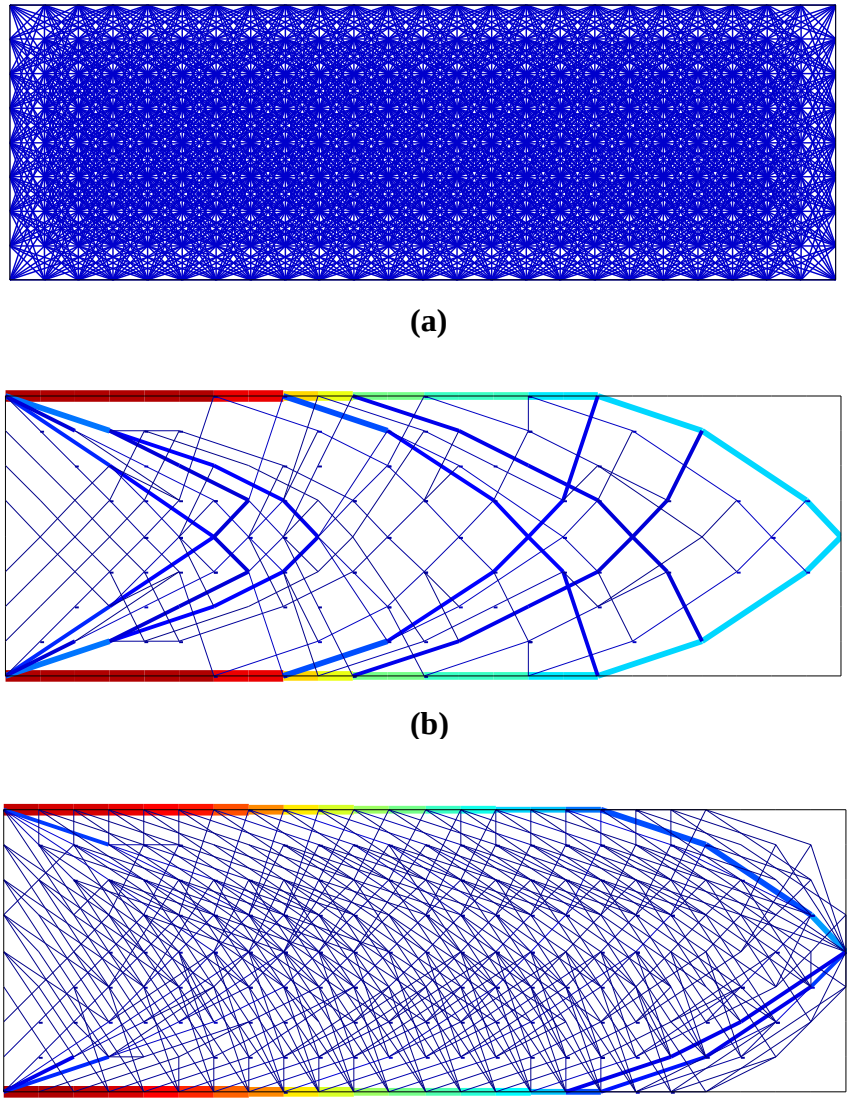

(a)

(b)

(c)

Figure 6.5: Comparison of final topologies for the cantilever beam problem using two-dimensional domain. (a) Ground structure with 24×8 mesh and level 3 connectivity, 2728 bars. (b) The optimal topology without instability consideration. (c) The final result with buckling consideration.

6.1.2 Three-dimensional cantilever beam

The cantilever beam problem is extended to three-dimensional domain. Boundary and load conditions are shown in Figure 6.6(a). The domain has dimensions with $L_x = 3$ and $L_y = L_z = 1$. The magnitude of the load is 1. The domain is discretized with $6 \times 2 \times 2$ mesh and level 4 connectivity (Figure 6.6(b)). There are 1418 bars in the ground structure. Figure 6.7 shows the comparison of optimal topologies between the implementation considering buckling and that not considering instability issue. The optimal topology without instability consideration is shown in Figure 6.7(a). Moreover, Figure 6.7(b) shows the final result with buckling consideration in the implementation. There is no long and slender bars in the final optimal topology with buckling consideration.

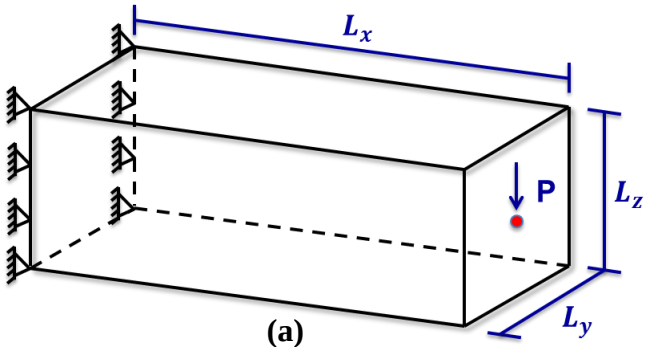

(a)

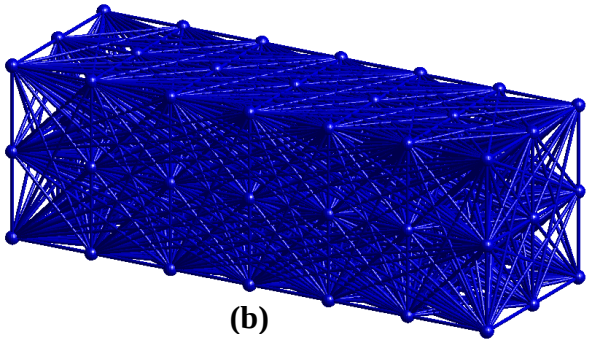

(b)

Figure 6.6: A cantilever beam problem in three-dimensional domain. (a) Dimensions, boundary and load conditions. (b) Ground structure with $6 \times 2 \times 2$ mesh, level 4 connectivity, 1418 bars.

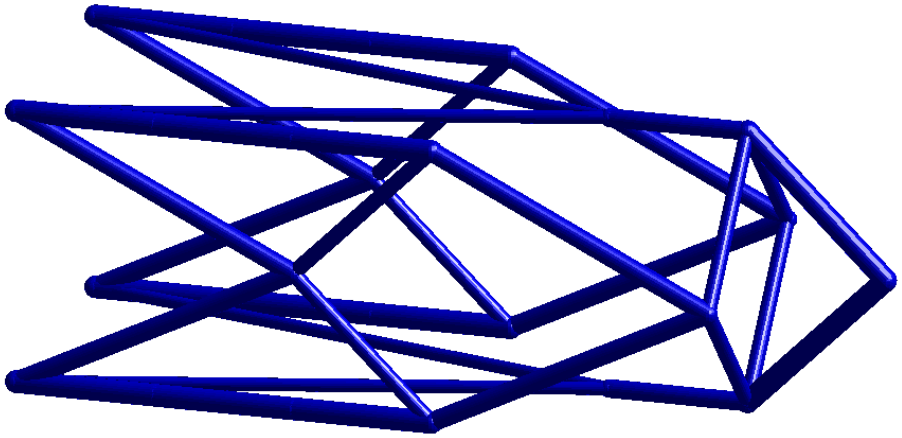

(a)

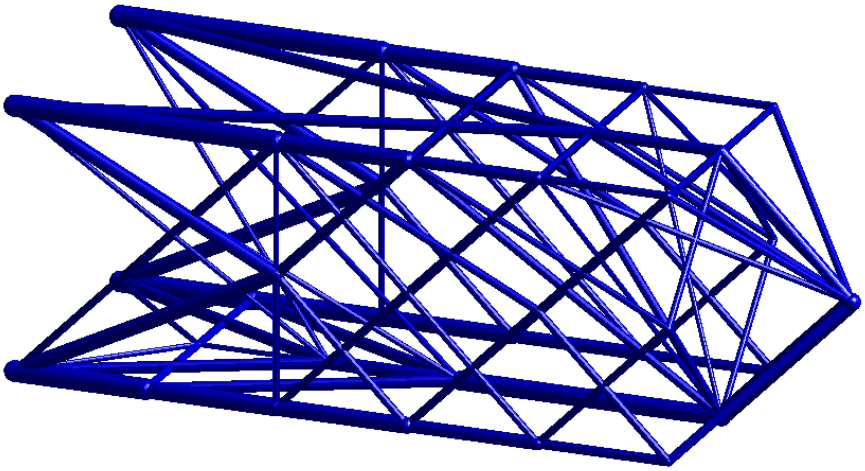

(b)

Figure 6.7: Comparison of the final topologies for the cantilever beam problem using three-dimensional domain. (a) The optimal topology without instability consideration. (c) The final result with buckling consideration in the implementation.

6.2 Examples with nodal instability only consideration

6.2.1 Two-dimensional column

The column is fixed at bottom, and loaded at the center of the top (Figure 6.8). The domain has dimensions with $L_x = 1$ and $L_y = 3$. The magnitude of the load is 1. The domain is discretized with 2×3 mesh and level 3 connectivity is used to generate the ground structure (Figure 6.9(a)). Figure 6.9(b) shows the optimum topology without instability consideration. There are several unstable nodes along the long bar. Figure 6.9(c) show the final topology obtained from the implementation considering nodal instability constraint. All the nodes in the structure are braced.

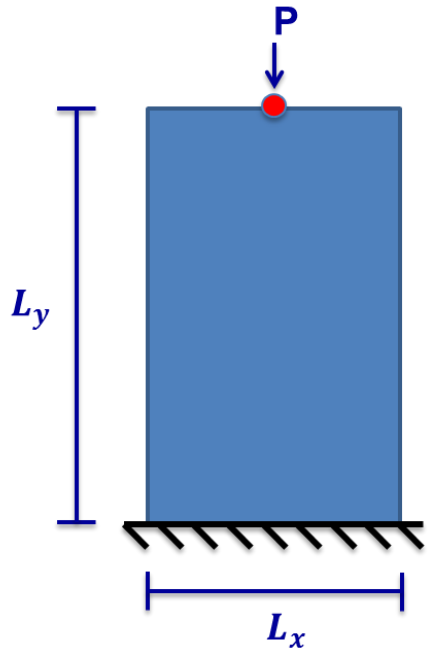

Figure 6.8: A column problem in two-dimensional domain

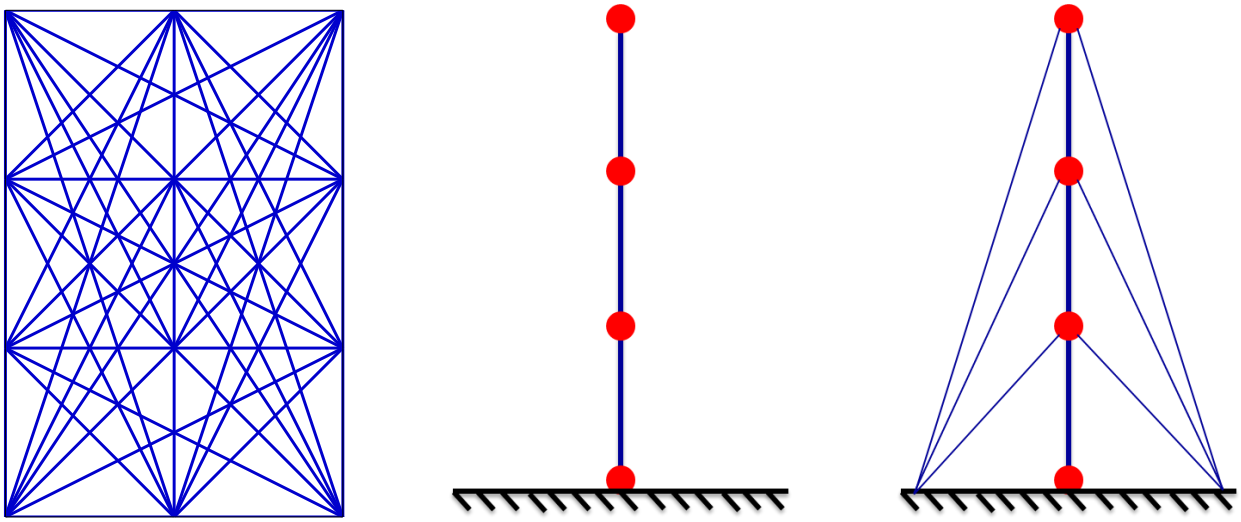

(a) **(b)** **(c)**

Figure 6.9: Comparison of final topologies for the column problem in two-dimensional domain. (a) Ground structure with 3×2 mesh and level 3 connectivity, 49 bars. (b) The optimal topology without instability consideration (c) The final result with nodal consideration in the implementation.

6.2.2 Three-dimensional column

The column problem is extended to a three-dimensional domain. The simple 3D tower problem by Tyas et al. (2006) is shown here. The domain has dimensions with $L_x = L_y = 2$ and $L_z = 10$. The magnitude of the load is 1. The domain is discretized with $2 \times 2 \times 10$ mesh and level 1 connectivity (Figure 6.10(b)). There are 710 bars in the ground structure. Figure 6.10(c) shows optimal topology obtained from the implementation considering nodal instability. There is no unstable nodes in the optimal structure.

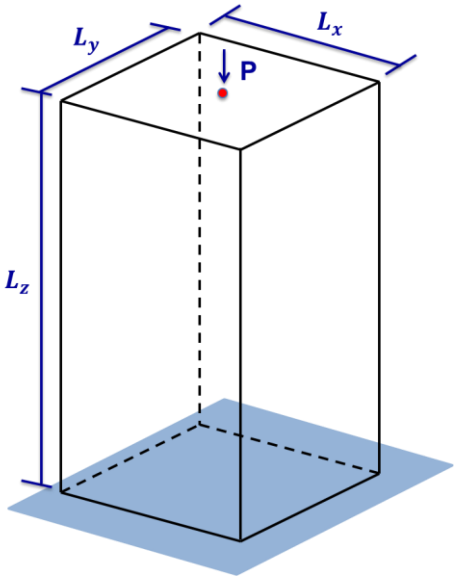

(a)

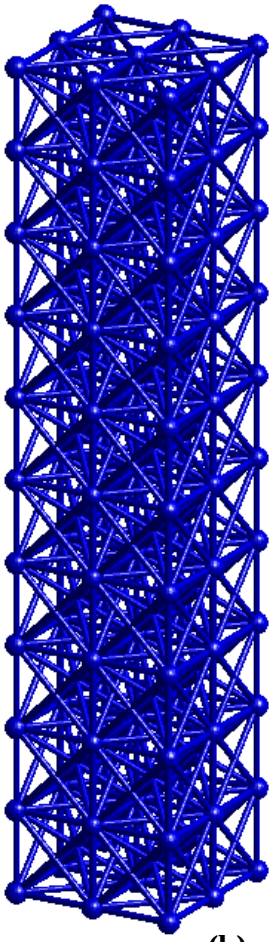

(b)

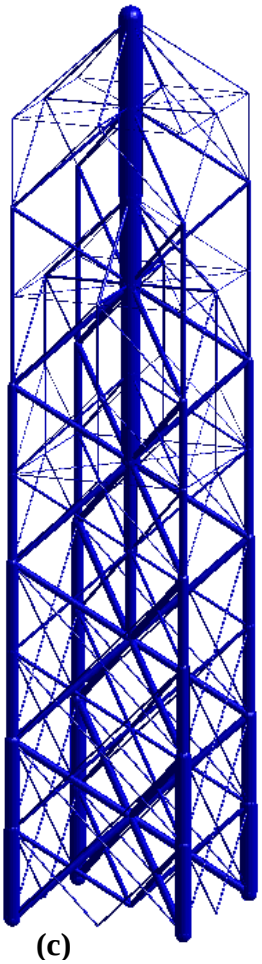

(c)

Figure 6.10: Tyas' simple column problem in three-dimensional domain. (a) Dimensions, boundary and load conditions. (b) Ground structure with $2 \times 2 \times 10$ mesh, level 1 connectivity, 710 bars.

6.3 An example with both buckling and nodal instability

A column example in three-dimensional domain is tested considering both buckling and nodal instability constraints. Figure 6.10 (a) shows the boundary and load conditions of the problem. The domain has dimensions with $L_x = L_y = 2$ and $L_z = 4$. The magnitude of the load is 1. The domain is discretized with $2 \times 2 \times 4$ mesh and level 4 connectivity (Figure 6.11(a)). There are 832 bars in the ground structure. Figure 6.11(b) shows the optimum topology with only buckling consideration. Figure 6.11(c) shows the optimum topology with only nodal instability consideration. Figure 6.11(d) shows the optimal topology obtained from the implementation considering both buckling and nodal instability constraints. This topology resembles some components of the previous two topologies.

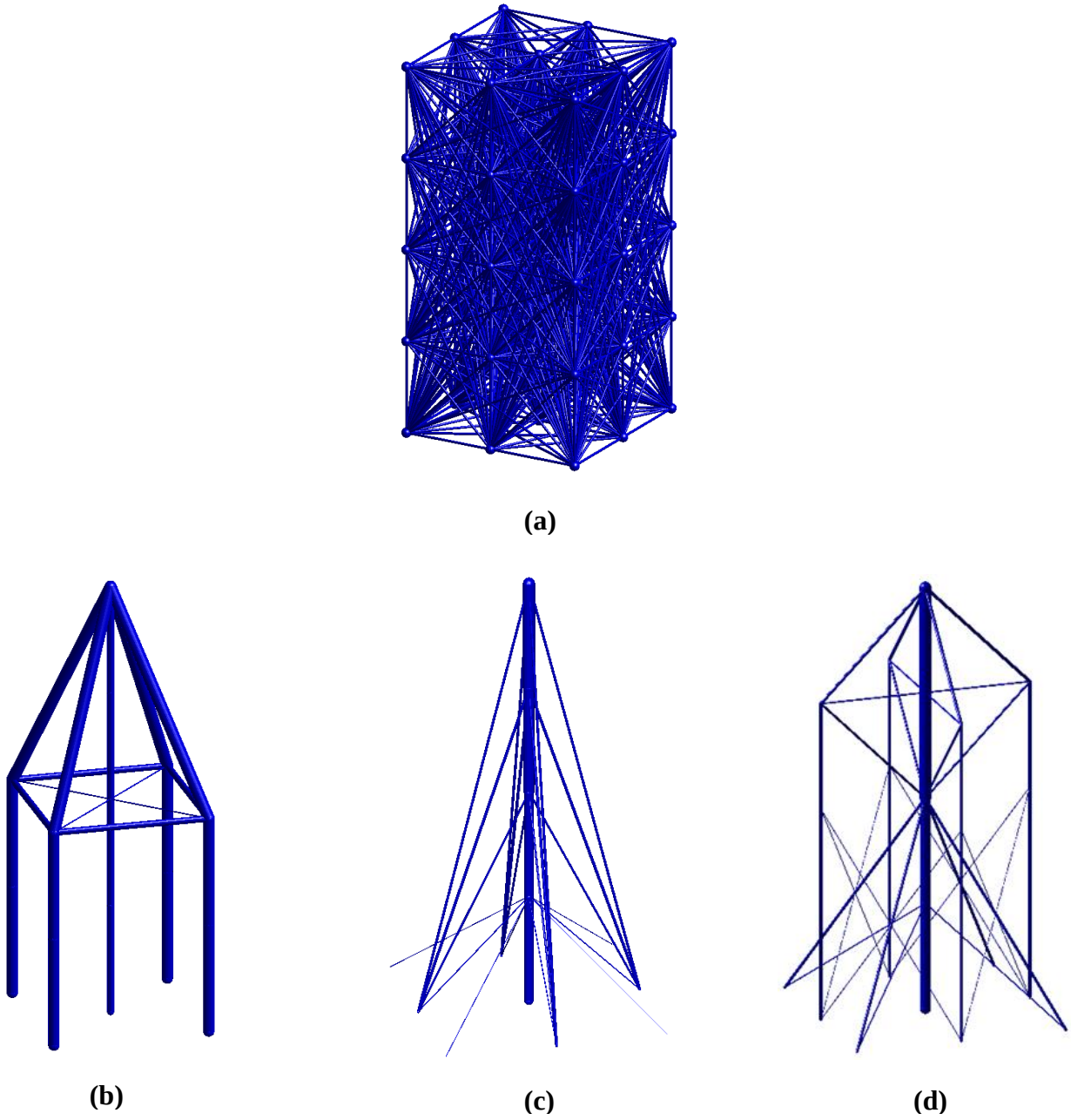

Figure 6.11: A three-dimensional column problem with instability consideration. (a) Ground structure with $2 \times 2 \times 4$ mesh and level 1 connectivity, 832 bars. (b) The optimal topology with buckling consideration. (c) The final result with nodal instability consideration. (d) The optimal topology with both buckling and nodal instability considerations.

Chapter 7 Conclusion

This thesis presents the development of the ground structure method involving both buckling and nodal instability considerations. The typical ground structure method using plastic formulation is reviewed. Then the ground structure method is implemented considering buckling constraint and nodal instability constraint either separately or in combination. This leads to three different implementation cases which is reasonable because real engineering problems might have different requirements. Thus the three implementations with different instability considerations give engineers options to solve relevant applied engineering problems. The Euler buckling criteria is taken as the buckling constraint in the implementation with local instability consideration. Nominal lateral force method (Tyas et al., 2006) is used in the implementation involving nodal instability consideration. The formulation with buckling consideration and the one with both local and nodal instability considerations are non-linear. Steps have been taken to improve the efficiency of the programing.

Numerical examples show the behavior and application of the implementations involving instability constraints. The problem domain can be both two-dimensional and three-dimensional. In the examples with buckling consideration only, a verification study was conducted. In addition, the optimum topology with buckling constraint was compared with that without instability consideration. There is no long and slender members in the optimal structure with buckling consideration. Moreover, every node in the optimal topologies with nodal instability consideration

are braced. No unstable nodes appear in those structures. In the example with both buckling and nodal instability consideration, the optimal structure shows features that can help the structural designer to avoid buckling and nodal instability issues. Next, a couple of suggestions for future work are highlighted.

7.1 Consideration of general domains

The present GS method could be extended to general three-dimensional restriction zones (Zegard and Paulino, 2014). This feature would allow consideration of more realistic structures (Beghini et al., 2014).

7.2 Extraction of structures out of the plastic ground structures

The final structure in the optimization process is obtained by setting a threshhold value on the areas. In order to connect this work with actual design and other fields of investigation, procedures need to be developed to ensure the local and global equilibrium satisfied for those structures.

References

Achtziger, W. (1999a). Local stability in the context of topology optimization - Part I: exact modelling. *Structural and Multidisciplinary Optimization*, 17:235-246.

Achtziger, W. (1999b). Local stability in the context of topology optimization – Part II: numerical approach. *Structural and Multidisciplinary Optimization*, 17:247-258.

Achtziger, W. (2007). On simultaneous optimization of truss geometry and topology. *Structural and Multidisciplinary Optimization*, 33:285-304.

Beghini, L. L., Beghini, A., Baker, W. F., and Paulino, G. H. (2010). Connecting architecture and engineering through structural topology optimization. *Engineering Structures*, 59:716-726.

Ben-Tal, A., Nemirovski, A. (1997). Robust truss topology design via semidefinite programming. *SIAM Journal on Optimization*, 7:991-1016.

Bendsoe, M. P., Sigmund, O. (2003). Topology optimization: theory, methods and applications. Engineering Online Library. Springer, Berlin, Germany, 2nd edition.

Descamps, B., Coelho, R. (2014). The nominal force method for the truss geometry and topology

optimization incorporating stability considerations. *Solids and Structures*. 51:2390-2399.

Dorn, W., Gomory, R., Greenberg, H. (1964). Automatic design of optimal structures. *Journal de Mecanique*, 3:25-52.

Gilbert, M., Tyas, A. (2003). Layout optimization of large-scale pin-jointed frames. *Engineering Computations*, 20:1044-1064.

Guo, X., Cheng, G., Olhoff, N. (2005). Optimum design of truss topology under buckling constraints. *Structural and Multidisciplinary Optimization*, 30:169-180.

Haftka, T. R., Gurdal, Z. (1992). Elements of structural optimization. Kluwer academic publishers, 3rd edition.

Hemp, W. S. (1973). *Optimum Structures*. Oxford University Press, Oxford, UK, 1st edition.

Karmarkar, N. (1984). A new polynomial-time algorithm for linear programming. *Combinatorica*, 4(4):373-395.

Kocvara, M. (2002). On the modelling and solving of the truss design problem with global stability constraints. *Structural and Multidisciplinary Optimization*. 23:189-203.

Pedersen, N.L., Nielsen, A.K. (2003). Optimization of practical trusses with constraints on eigenfrequencies, displacements, stresses and buckling. *Structural and Multidisciplinary Optimization*. 25:436-445.

Rozvany, G.I.N. (1996). Difficulties in truss topology optimization with stress, local buckling and system stability constraints. *Structural and Multidisciplinary Optimization*, 17:235-246.

Sokol, T. (2011). A 99 line code for the discretized Michell truss optimization written in Mathematica. *Structural and Multidisciplinary Optimization*, 43(2): 181-190.

Tyas, A., Gilbert, M., Pritchard, T. (2006). Practical plastic layout optimization of trusses incorporating stability considerations. *Computers Structures*. 84:115-126.

Winter, G. (1958). Lateral bracing of columns and beams. Proc ASCE. 1561:1-22.

Wright, M. H. (2004). The interior-point revolution in optimization: history, recent developments, and lasting consequences. *Bulletin of the American Mathematical Society*, 42(1):39-56.

Zegard, T., Paulino, G.H. (2014). GRAND — Ground structure based topology optimization for arbitrary 2D domains using MATLAB. *Structural and Multidisciplinary Optimization.* 50(5):861-882.

Zhou, M. (1996). Difficulties in truss topology optimization with stress and local buckling constraints. *Structural and Multidisciplinary Optimization*. 11:134-136.